ChemPubSoc Europe

DOI: 10.1002/open.201600155

Open Access ChemistryOPEN Communications

An Approach Toward Replacing Vanadium: A Single Organic Molecule for the Anode and Cathode of an Aqueous Redox-Flow Battery

Tobias Janoschka,[a, b] Christian Friebe,[a, b] Martin D. Hager,[a, b] Norbert Martin,[c] and Ulrich S. Schubert*[a, b]

By combining a viologen unit and a 2,2,6,6-tetramethylpiperidin-1-oxyl (TEMPO) radical in one single combi-molecule, an artificial bipolar redox-active material, 1-(4-(((1-oxyl-2,2,6,6-tetramethylpiperidin-4-yl)oxy)carbonyl)benzyl)-1′-methyl-[4,4′-bipyridine]-1,1′-diium-chloride (**VIOTEMP**), was created that can serve as both the anode (−0.49 V) and cathode (0.67 V vs. Ag/AgCl) in a water-based redox-flow battery. While it mimics the redox states of flow battery metals like vanadium, the novel aqueous electrolyte does not require strongly acidic media and is best operated at pH 4. The electrochemical properties of **VIOTEMP** were investigated by using cyclic voltammetry, rotating disc electrode experiments, and spectroelectrochemical methods. A redox-flow battery was built and the suitability of the material for both electrodes was demonstrated through a polarity-inversion experiment. Thus, an organic aqueous electrolyte system being safe in case of cross contamination is presented.

By the end of 2014, renewable power plants amounted to over a quarter of the global power-generating capacity. Rapidly falling costs led to the installation of 40 GW photovoltaic (PV) and 51 GW wind farms in 2014 alone. With the massive proliferation of renewables, the demand of large-scale energy-storage systems increases to mitigate the problems that come with a fluctuating energy production.[1] Although extremely compact Li-ion batteries with high energy and power densities have become the standard for portable applications, the deployment of large stationary batteries is still in its early stages. The focus in this field is on inexpensive, safe, reliable, environmentally friendly, and long-lasting storage solutions. Although conventional battery systems, like lead-acid, nickel-metal hydride, or Li-ion batteries, are employed, great attention is drawn to redox-flow batteries (RFBs).[2] RFBs are superior to conventional capsuled batteries, as their working principle allows them to be easily scaled to fit the needs of virtually every application, from domestic use to large wind farms. In contrast to the usual solid-state electrodes, the redox-active material of an RFB is dissolved and stored in an electrolyte reservoir, which determines the battery's capacity. Upon charging/discharging, the electrolyte is transported through an electrochemical reactor (cell stack), where the redox reactions take place. Hence, the power output can be tailored as a function of the number of cell stacks.

Among the multitude of redox chemistries, the most widely commercialized system is the all-vanadium RFB. This intensively studied battery uses vanadium salts in sulfuric acid as the electrolyte solution for both the anode and the cathode. Besides multivalent vanadium ($V^{3+}/V^{2+}//VO_2^+/VO^{2+}$), chromium ($Cr^{3+}/Cr^{2+}//CrO_4^{2-}/Cr^{3+}$), neptunium ($Np^{4+}/Np^{3+}//NpO_2^{2+}/NpO_2^+$), and even uranium have also been investigated. These systems stand out from all other RFBs, because they use the same metal ion in different oxidation states as the anode and cathode material. In case the redox-active species cross the membrane, which separates the anode and cathode, the battery can be rebalanced easily without any harm being done to the RFB. In contrast, two-component systems (e.g. zinc/bromine or iron/chromium) can be severely damaged by cross contamination.[2c, d, 3]

Beside metal-based RFBs, the usage of organic materials has recently attained much attention, because they can be prepared at low cost from an abundant resource basis and allow the redox potential to be tailored through organic synthesis. These systems use either organic solvents (e.g. Li/anthraquinone,[4] Li/TEMPO,[3b] thiophene,[5] Li/viologen,[6] quinoxaline/2-dialkyl-oxy benzene[7]) or acidic electrolytes (e.g. Br_2/anthraquinone,[8] quinone/anthraquinone[9]) and generally two different materials for the anode and cathode. Although organic systems suffer from a low power density, owing to a low ion mobility, the acidic electrolytes are highly corrosive.

To approach the problems associated with cross contamination in an organic two-component RFB, we present a novel approach to mimic the behavior of vanadium or chromium RFBs by using an artificial bipolar organic material that can be used in an aqueous electrolyte solution.

Although the number of intrinsically bipolar materials is very limited and often does not fit the voltage window suitable for

[a] T. Janoschka, Dr. C. Friebe, Dr. M. D. Hager, Prof. Dr. U. S. Schubert
Friedrich Schiller University Jena
Laboratory of Organic and Macromolecular Chemistry (IOMC)
Humboldtstraße 10, 07743 Jena (Germany)
E-mail: ulrich.schubert@uni-jena.de

[b] T. Janoschka, Dr. C. Friebe, Dr. M. D. Hager, Prof. Dr. U. S. Schubert
Center for Energy and Environmental Chemistry Jena (CEEC Jena)
Philosophenweg 7a, 07743 Jena (Germany)

[c] Dr. N. Martin
JenaBatteries GmbH
Botzstraße 5, 07743 Jena (Germany)

Supporting Information for this article can be found under: http://dx.doi.org/10.1002/open.201600155.

aqueous solutions,[5,10] various organic redox-active compounds with only one redox reaction are known.[11]

By covalently linking a 4-hydroxy-2,2,6,6-tetramethylpiperidin-1-oxyl (TEMPOL) free radical—a cathode material—with a *N*,*N*′-dialkyl-4,4′-bipyridinium (viologen) moiety—an anode material—the bipolar combi-molecule **VIOTEMP** was created. The redox potentials of both individual compounds are compatible with aqueous systems, rendering them suitable candidates for a bipolar material.[12]

For linking TEMPOL (**1**) with the viologen unit, a benzyl linker was introduced with good yield through the esterification of **1** with 4-(chloromethyl)benzoyl chloride **2** at room temperature (Scheme 1). Upon conversion with 4,4′-bipyridine in

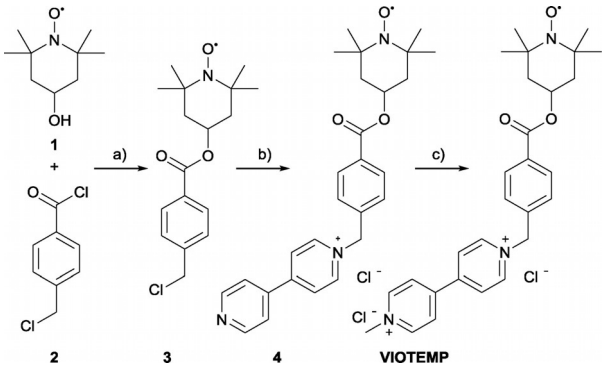

Scheme 1. Schematic representation of the synthesis of the bipolar, redox-active material **VIOTEMP**. Reagents and conditions: a) dry dichloromethane, dry triethylamine, 25 °C, 5 h, yield (**3**): 88%; b) acetonitrile, 4,4′-bipyridine, 80 °C, 72 h, yield (**4**): 74%; c) dimethyl sulfoxide, methyl iodide, 60 °C, 2 h, ion exchange with DOWEX Marathon A2, yield (**VIOTEMP**): 64%.

acetonitrile at 80 °C, precursor **4** was obtained. In addition to acetonitrile (yield: 74%), chloroform (35%), butyronitrile (76%), chlorobenzene (58%), and dimethyl sulfoxide (57%) were tested as the solvent. For the second functionalization step, **4** was reacted with methyl iodide, followed by an ion exchange to the electrochemically more stable chloride ion, finally yielding the redox-active material.

VIOTEMP was analyzed by using cyclic voltammetry (CV). Representative voltammograms are displayed in Figure 1 and show the oxidation of the TEMPO· radical to its corresponding oxoammonium salt $TEMPO^+$ as well as the reduction of the divalent viologen cation ($Viol^{++}$) to the monovalent radical cation ($Viol^{+\cdot}$). A second redox step, forming the neutral viologen ($Viol^0$), was not studied in detail, as it appeared to be irreversible and is, therefore, not suitable for battery application.

In agreement with previous findings,[11f] the viologen reduction occurs at −0.49 V (vs. Ag/AgCl) and the TEMPO oxidation at 0.67 V. This results in a theoretical cell voltage of 1.16 V. Both reactions reveal a quasireversible behavior with a linear correlation between peak current and the square root of the scan rate, indicating diffusion-controlled behavior (Figure S4 and S5). A small shoulder at about −0.35 V may be attributed to the reduction of the TEMPO· radical to its hydroxylamine form (TEMPO-NOH).[13] To further clarify the anodic redox processes, spectroelectrochemical measurements using electron

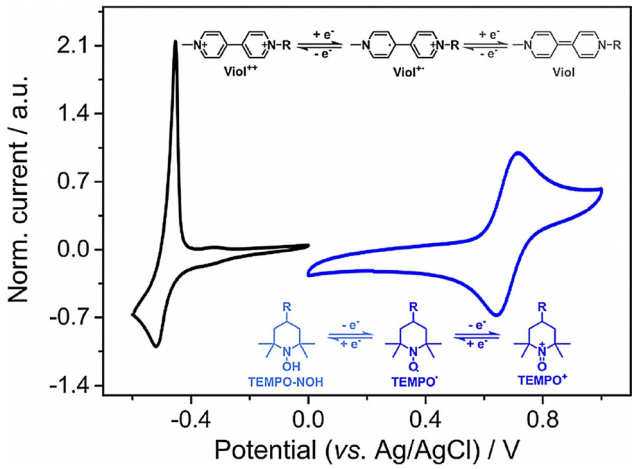

Figure 1. Cyclic voltammograms of **VIOTEMP** (1 g L^{-1}) in sodium chloride solution (0.5 mol L^{-1}), scan rate 200 mV s^{-1}.

paramagnetic resonance (EPR) as well as UV/Vis spectroscopy were employed (Figure S6 to S8). The time-dependent UV/Vis spectra acquired at a potential of −0.9 V (vs. Ag/AgCl) show, in a first step, only the formation of a species absorbing at 385 nm. A second species is subsequently formed featuring an additional strong absorption between 480 to 780 nm. While the latter corresponds to the viologen radical cation ($Viol^{+\cdot}$),[14] the first is indicative for the reduction of TEMPO·. Further confirmation is found in the EPR spectrum after electrolysis at −0.9 V (vs. Ag/AgCl). It reveals the complete disappearance of the typical TEMPO· radical signal, followed by the formation of a signal set attributed to the viologen radical cation ($Viol^{+\cdot}$).

The kinetics of the redox reactions were studied by using rotating-disc-electrode (RDE) experiments (Figures S9 and S10). For the $Viol^{++}$ and the TEMPO· reduction processes, a peak was observed even at high rotation speeds (4900 rpm) and within a broad scan-rate window (1 to 50 mV s^{-1}). Being indicative for the depletion of reactive species at the electrode surface, this behavior is most likely caused by the overlapping of the two redox reactions and impedes further analysis of the voltammograms. However, by Levich analysis of the RDE voltammograms of the TEMPO· oxidation, the diffusion coefficient D was determined by the Levich equation [Eq. (1)] to be $D = 2.9\times10^{-4}$ $cm^2\,s^{-1}$:

$$i_{lim} = 0.62nFAD^{\frac{2}{3}}\omega^{\frac{1}{2}}\nu^{-\frac{1}{6}}c_0, \quad (1)$$

with i_{lim} being the limiting current, ω the rotation speed, c_0 the bulk concentration of the analyte, $n = 1$ the number of transferred electrons, $F = 96\,485$ C mol^{-1} Faraday's constant, $A = 0.196$ cm^2 the electrode surface, and $\nu = 1.01\times10^{-6}$ $m^2\,s^{-1}$ the kinematic viscosity of an aqueous sodium chloride solution (0.1 mol L^{-1}). Subsequently, the mass-transfer-independent kinetic current i_k was obtained by using the Koutecký–Levich equation [Eq. (2)]:

$$\frac{1}{i} = \frac{1}{i_k} + \frac{1}{0.62nFAD^{\frac{2}{3}}\omega^{\frac{1}{2}}\nu^{-\frac{1}{6}}c_0}, \quad (2)$$

and fitted by the Butler–Volmer equation through a Tafel plot to yield i_0 and, eventually, the electron-transfer rate constant $k^0 = 5.8 \times 10^{-2}$ cm s^{-1} as well as the transfer coefficient $\alpha = 0.55$ by using Equation (3):

$$i_0 = FAk^0c_0 \quad (3)$$

and Equation (4):

$$\text{Tafel slope} = \frac{(1-\alpha)F}{2.3RT} \quad (4)$$

The general performance of the active material in an RFB was studied by using an aqueous solution of **VIOTEMP** (25 mmol L^{-1}) in a volume ratio of catholyte to anolyte of 2:1 (20 mL:10 mL). A setup consisting of a peristaltic pump, two electrolyte reservoirs, and a 5 cm^2 test cell was used for the constant current cycling tests. Sodium chloride (0.3 mol L^{-1}) was employed as supporting electrolyte, owing to its good stability in the applied potential window, its low toxicity, and its compatibility with the used anion-exchange membranes. During the first charging of the battery, two processes occur in the anolyte. First, TEMPO· is reduced to its hydroxylamine form TEMPO-NOH, resulting in a charging plateau at approximately 0.9 V. This preconditioning step is followed by the reduction of Viol^{++} to Viol$^{+\cdot}$, as indicated by a color change from orange to violet and resulting in a second charging plateau at approximately 1.2 V (Figure S11). At the same time, two equivalents of TEMPO· are oxidized to TEMPO$^+$ in the catholyte. Exploiting the redox couples TEMPO$^+$/TEMPO· and Viol^{++}/Viol$^{+\cdot}$, the battery can be cycled repeatedly at the voltage of the second plateau. The preconditioning step forming TEMPO-NOH could also be performed by using any other sacrificial substance instead of the catholyte itself. To study the bipolar functionality of **VIOTEMP**, the battery was fully charged and, subsequently, the portion of catholyte used as sacrificial agent (50%; 10 mL) was removed. Afterwards, the current regime could be inverted numerous times in a polarity-inversion experiment (Figure 2). Upon inversion of the charging and discharging currents, a full reversal of the system's behavior was observed, including voltage profiles and the color of the solutions.

Although **VIOTEMP** shows a high solubility in water, it became apparent that the less polar, reduced radical cation (Viol$^{+\cdot}$) precipitates from electrolyte solutions at concentrations above 25 mmol L^{-1}. For this reason, 20 vol% ethylene carbonate, an electrochemically inert organic solvent, was added to adjust the solution characteristics of the electrolyte and stabilize **VIOTEMP** in all applied redox states at a concentration of 0.1 mol L^{-1}. Other tested additives, like dimethyl sulfoxide and acetonitrile, led to membrane damage or a fast capacity fade.

As the pH value of the electrolyte solution changes considerably during the charging of the battery, owing to the reduction of TEMPO· to its hydroxylamine form TEMPO-NOH, acetate buffer and phosphate buffer (pH ≈ 4) were evaluated as additives to compensate the change in proton concentration. Both buffers are compatible with the electrolyte solution and sufficiently stabilize the pH value between 2.5 and 7. At higher pH values, Viol^{++} and TEMPO$^+$ decompose, whereas, at lower pH values, TEMPO· undergoes a disproportionation reaction.

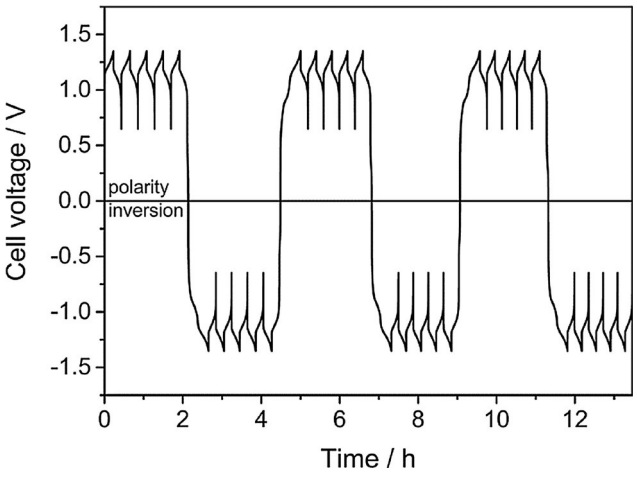

Figure 2. Polarity-inversion test of a pumped redox-flow battery at 5 mA cm^{-2}. The cell polarity was changed after five repeated charging/discharging cycles by inverting the applied current regime (25 mmol L^{-1} **VIOTEMP** in 0.3 mol L^{-1} aqueous NaCl).

In addition, several anion-exchange membranes were evaluated (FAA3-50, FAP-PK3130, FAPQ-3100-PF, and FAS-30, all provided by FUMATECH BWT GmbH, Germany) in terms of their influence on cell resistance and stability through repeated charge/discharge cycling at 10 mA cm^{-2} (Table S1). FAA3-50 and FAS-30, both non-reinforced anion-exchange membranes on a PET carrier, led to the lowest area-specific cell resistance (1.85 and 1.52 Ω cm^2). However, extended cycling of electrolytes containing additive and buffer showed a gradual decrease in capacity, starting between the fifth and the tenth cycle after an initial increase to the theoretical capacity had been observed (Figure S12).

In conclusion, artificial bipolar combi-molecule **VIOTEMP** was prepared and used to construct a "pole-less" aqueous RFB. The material covalently links a TEMPO radical with a viologen moiety, allowing for three redox couples, of which two are exploited for energy storage. The battery can be reversibly cycled and the polarity easily changed, as the same material is used for both electrodes. Although the capacity is still limited by the solubility of the reduced species, an improvement in the performance is anticipated upon introduction of a more hydrophilic linker unit. Allowing for a simplified rebalancing process, which is often necessary in commercial RFBs, and preventing damage or capacity fade caused by cross-contamination as observed in asymmetrically built batteries, the concept of combi-molecules, whose redox potential can be tailored to fit the potential window of water-based electrolytes, may pave the way for the replacement of (heavy-)metal-based RFB electrolytes.

Experimental Section

Reagents and Instruments

All reagents were bought from Sigma–Aldrich, AlfaAesar, or TCI and used as received without further purification. ^{1}H NMR spectra were measured on a FOURIER 300 from Bruker at 25 °C, *J* values are given in Hz. ATR-FTIR spectra were acquired on a Nicolet Avatar 370 DTGS (Thermo Electron Corp., USA). X-band EPR spectra were acquired on an EMXmicro CW-EPR spectrometer from Bruker, Germany (EMX micro EMM-6/1/9-VT control unit, ER 070 magnet, EMX premium ER04 X-band microwave bridge equipped with EMX standard resonator, EMX080 power unit) using powdered samples. The samples were investigated at room temperature and the data handling was done on the Bruker Xenon software package, version 1.1b86. The SpinCount™ software module was used for quantitative measurements.

ESI-Q-TOF MS measurements (positive-ion mode) were performed by using a micrOTOF mass spectrometer (Bruker Daltonics, Germany) equipped with an automatic syringe pump by KD Scientific for sample injection. The standard electrospray ion (ESI) source was used to generate the ions and the instrument was calibrated in the *m/z* range 50 to 3000 by using an internal calibration standard (Tunemix solution, Agilent, USA). Sample concentrations ranging from 1 to 10 mg mL^{-1} were injected by using a constant flow (3 mL min^{-1}) of sample solution. Data and HRMS calculations were processed through the Bruker Data Analysis software version 4.0.

CV and RDE experiments were conducted on an SP-50 potentiostat/galvanostat (Bio-Logic, France). For CV, a standard three-electrode setup with a glassy-carbon-disk working electrode (2 mm diameter), a Ag/AgCl/water reference electrode, and a platinum-wire counter electrode were used. For RDE studies, a glassy-carbon-disk working electrode with a diameter of 5 mm was employed and the rotation speed of an EDI101 rotator was controlled by a CTV101 (Radiometer analytical, France).

EPR spectroelectrochemical measurements were conducted in an ER164EC-Q electrolytic cell assembly (Bruker, Germany) equipped with platinum wires as working and counter electrode as well as a Ag/AgCl/water reference electrode in potentiostatic mode. The redox process was monitored by using an EMXmicro CW-EPR spectrometer (Bruker, Germany). The analytes were dissolved in aqueous solutions of sodium chloride (0.5 mol L^{-1}) at concentrations of 10^{-4} mol L^{-1}.

UV/Vis spectroelectrochemical measurements were conducted in a quartz cuvette (1 mm optical path length) equipped with a platinum-grid working electrode, a platinum-wire auxiliary electrode, and a Ag/AgCl/water reference electrode in potentiostatic mode. The redox process was monitored by UV/Vis spectroscopy using a Lambda 750 UV/Vis spectrophotometer (PerkinElmer, USA) and considered complete when there was no further spectral change. The analytes were dissolved in aqueous solutions of sodium chloride (0.5 mol L^{-1}) at concentrations of 10^{-2} mol L^{-1}.

Charging/discharging tests were carried out at 25 °C by using a potentiostat (VMP3, Biologic, France), a peristaltic pump at a flow rate of 20 mL min^{-1} (Hei-FLOW Advantage, Heidolph, Germany), and an RFB test cell (Jenabatteries GmbH, Germany): PTFE frame, PTFE seals, graphite current collectors, graphite felt electrodes (2.25 × 2.25 × 0.4 cm^3, GFA6, SGL, Germany), active area of 5 cm^{-2}. The battery was charged/discharged under a constant-current regime. Aqueous electrolyte solution (0.1 mol L^{-1} **VIOTEMP**, 0.3 mol L^{-1} NaCl, 20 vol% ethylene carbonate in 0.4 mol L^{-1} phosphate buffer at pH ≈ 4) was employed as the anolyte (10 mL) and catholyte (20 mL). All electrolyte solutions were kept under an argon atmosphere. To perform the polarity-inversion test, the battery was first fully charged at 5 mA cm^{-2}. Afterward, half of the catholyte solution (10 mL) was removed with a syringe and, subsequently, the polarity was inverted by changing the current regime to −5 mA cm^{-2}. Stability tests of membrane materials (anion-exchange membranes FAA3-50, FAP-PK3130, FAPQ-3100-PF, and FAS-30 by FUMATECH BWT GmbH, Germany) and additives (dimethyl sulfoxide, ethylene carbonate, and acetonitrile) were performed by repeatedly charging/discharging a test cell at 10 mA cm^2.

1-Oxyl-2,2,6,6-tetramethylpiperidine-4-yl-4-(chloromethyl)-benzoate (3)

To a solution of 4-hydroxy-2,2,6,6-tetramethylpiperidine-*N*-oxyl **1** (30 g; 174 mmol) in dry dichloromethane (240 mL) and dry trimethylamine (48 mL) under an argon atmosphere, 4-(chloromethyl)-benzoyl chloride **2** (26 mL; 183 mmol) was added dropwise under stirring, while the temperature was monitored and kept below 30 °C by cooling with an ice bath. After 5 h at room temperature, the reaction mixture was poured onto ice water (500 mL) containing an aqueous solution of sodium hydrogen carbonate (5%; 300 mL). The organic phase was collected and washed with water (3 × 100 mL), dried over magnesium sulfate, and the solvent was removed in vacuo. After drying (10^{-2} bar, 25 °C), the crude product (49.9 g, 88%) was obtained as a yellow powder and used without any further purification.

^{1}H NMR (300 MHz, [D$_6$]DMSO) δ = 7.94 (d, *J* = 8.2 Hz, 2H), 7.57 (d, *J* = 8.3 Hz, 2H), 5.18 (m, 1H), 4.83 (s, 2H), 1.97 (m, 2H), 1.59 (m, 2H), 1.12 ppm (s, 12H), (quenched with phenylhydrazine); ATR-FTIR (solid): $\tilde{\nu}$ = 3002 (w), 2971 (w), 2933 (w), 1714 (s), 1612 (m), 1463 (w), 1444 (w), 1415 (m), 1365 (m), 1313 (m), 1274 (s), 1241 (s), 1180 (s), 1118 (s), 1020 (m), 979 (m), 962 (m), 854 (m), 817 (m), 798 (m), 771 8 m), 709 (s), 678 (m), 566 (m), 512 ppm (m); m.p. 119–121 °C; HRMS (ESI): *m/z* calcd for $C_{17}H_{23}ClNO_3$: 324.1360 $[M]^+$; found, 324.1353.

1-(4-(((1-Oxyl-2,2,6,6-tetramethylpiperidine-4-yl)oxy)carbonyl)benzyl)-[4,4′-bipyridin]-1-ium-chloride (4)

The crude product **3** (48 g; 148 mmol) and 4,4′-bipyridine (23.1 g; 148 mmol) were dissolved in acetonitrile (800 mL) under an argon atmosphere and the solution was subsequently stirred at 80 °C for 72 h. The reaction mixture was precipitated in cold ethyl acetate (2 L), the precipitate collected on a sintered glass filter and washed with cold ethyl acetate (250 mL). After drying (10 mbar, 40 °C), the title compound (52.7 g, 74%) was obtained as an orange powder.

^{1}H NMR (300 MHz, [D$_6$]DMSO) δ = 9.41 (d, *J* = 6.7 Hz, 2H), 8.86 (d, *J* = 5.9 Hz, 2H), 8.67 (d, *J* = 6.8 Hz, 2H), 8.00 (m, 4H), 7.71 (d, *J* = 8.1 Hz, 2H), 6.02 (s, 2H), 5.17 (m, 1H), 1.95 (m, 2H), 1.59 (m, 2H), 1.11 ppm (s, 12H), (quenched with phenylhydrazine); ATR-FTIR (solid): $\tilde{\nu}$ = 3116 (w), 3009 (w), 2989 (m), 2973 (m), 2933 (w), 1712 (s), 1637 (s), 1612 (m), 1527 (m), 1492 (m), 1463 (m), 1415 (m), 1373 (m), 1315 (m), 1274 (s), 1241 (m), 1226 (m), 1178 (m), 1157 (s), 1110 (s), 1099 (m), 1025 (m), 979 (m), 871 (w), 821 (m), 800 (s), 773 (m), 734 (s), 715 (s), 642 (w), 559 (m), 514 (m), 466 ppm (m); m.p. decomposition > 200 °C; HRMS (ESI): *m/z* calcd for $C_{27}H_{31}N_3O_3$: 445.2359 $[M-Cl]^+$; found, 445.2357.

1-(4-(((1-Oxyl-2,2,6,6-tetramethylpiperidin-4-yl)oxy)carbonyl)benzyl)-1′-methyl-[4,4′-bipyridine]-1,1′-diium-chloride (VIOTEMP)

A solution of **4** (5.0 g; 10.4 mmol) and methyl iodide (1.3 mL; 20.8 mmol) in dimethyl sulfate (100 mL) was stirred at 60 °C for 2 h until complete consumption of the educt according to TLC (acetonitrile/water/KNO_3; 10/1/0.1). After cooling the solution to room temperature, it was poured into cold ethyl acetate (500 mL). The precipitate was collected on a sintered glass filter and washed with ethyl acetate (2×25 mL). After drying (10 mbar, 40 °C), the crude product was refluxed in ethyl acetate (500 mL) two times for 2 h to remove impurities. The solids were collected on a sintered glass filter, washed with ethyl acetate (2×25 mL), and dried (10^{-3} mbar, 25 °C), obtaining an orange powder (6.15 g, 95%).

An ion exchange from iodide to chloride was carried out by using DOWEX Marathon A2 (chloride form) ion-exchange resin (3.5 g, 64%).

A portion of the product was purified through column chromatography (acetonitrile/water/KNO_3; 10/1/0.1) for HR-ESI-MS measurements.

^{1}H NMR (300 MHz, D_2O) $\delta = 9.02$ (dd, $J = 4.4$, 56.4 Hz, 4H), 8.44 (dd, $J = 4.4$, 21.3 Hz, 4H), 8.03 (d, $J = 8.2$ Hz, 2H), 7.51 (d, $J = 8.2$ Hz, 2H), 5.92 (s, 2H), 5.26 (m, 1H), 4.40 (s, 3H), 2.05 (pd, $J = 12.9$ Hz, 2H), 1.71 (pt, $J = 11.7$ Hz, 2H), 1.16 ppm (m, 12H), (quenched with phenylhydrazine); ATR-FTIR (solid): $\tilde{\nu} = 3365$ (br; H_2O), 3106 (m), 3035 (m), 2975 (m), 2973 (m), 2863 (w), 1712 (s), 1635 (s), 1614 (m), 1558 (m), 1506 (m), 1446 (m), 1415 (m), 1361 (m), 1315 (m), 1272 (s), 1241 (m), 1178 (m), 1178 (s), 1105 (s), 1020 (m), 979 (w), 964 (w), 835 (m), 804 (m), 761 (s), 717 (s), 703 (m), 642 (w), 553 (m), 489 ppm (m); m.p. decomposition >200 °C; degree of oxidation: 96% (EPR); HRMS (ESI): *m/z* calcd for $C_{28}H_{33}N_3O_3$: 459.2516 $[M-H]^+$; found, 459.2498.

Acknowledgements

The authors acknowledge the Federal Ministry for Economic Affairs and Energy (BMWi), the Central Innovation Programme for SMEs (ZIM), the European Social Fund (ESF), the Thüringer Aufbaubank (TAB), the Thuringian Ministry for Economic Affairs, Science and Digital Society (TMWWdG), and the Fonds der Chemischen Industrie (FCI) for financial support. We thank Maria Strumpf and Kristin Schreyer for their assistance in the preparation of the redox-active materials.

Keywords: cyclic voltammetry · electrochemistry · redox-flow batteries · TEMPO · viologen

[1] REN21, *Renewables 2015 Global Status Report*, REN21 Secretariat, Paris, **2015**.
[2] a) Z. Yang, J. Zhang, M. C. W. Kintner-Meyer, X. Lu, D. Choi, J. P. Lemmon, J. Liu, *Chem. Rev.* **2011**, *111*, 3577–3613; b) B. Dunn, H. Kamath, J. M. Tarascon, *Science* **2011**, *334*, 928–935; c) P. Alotto, M. Guarnieri, F. Moro, *Renew. Sust. Energ. Rev.* **2014**, *29*, 325–335; d) J. Noack, N. Roznyatovskaya, T. Herr, P. Fischer, *Angew. Chem. Int. Ed.* **2015**, *54*, 9776–9809; *Angew. Chem.* **2015**, *127*, 9912–9947.
[3] a) W. Wang, Q. T. Luo, B. Li, X. L. Wei, L. Y. Li, Z. G. Yang, *Adv. Funct. Mater.* **2013**, *23*, 970–986; b) X. Wei, W. Xu, M. Vijayakumar, L. Cosimbescu, T. Liu, V. Sprenkle, W. Wang, *Adv. Mater.* **2014**, *26*, 7649–7653.
[4] W. Wang, W. Xu, L. Cosimbescu, D. W. Choi, L. Y. Li, Z. G. Yang, *Chem. Commun.* **2012**, *48*, 6669–6671.
[5] S. H. Oh, C. W. Lee, D. H. Chun, J.-D. Jeon, J. Shim, K. H. Shin, J. H. Yang, *J. Mater. Chem. A* **2014**, *2*, 19994–19998.
[6] G. Nagarjuna, J. S. Hui, K. J. Cheng, T. Lichtenstein, M. Shen, J. S. Moore, J. Rodriguez-Lopez, *J. Am. Chem. Soc.* **2014**, *136*, 16309–16316.
[7] F. R. Brushett, J. T. Vaughey, A. N. Jansen, *Adv. Energy Mater.* **2012**, *2*, 1390–1396.
[8] B. Huskinson, M. P. Marshak, C. Suh, S. Er, M. R. Gerhardt, C. J. Galvin, X. D. Chen, A. Aspuru-Guzik, R. G. Gordon, M. J. Aziz, *Nature* **2014**, *505*, 195–198.
[9] B. Yang, L. Hoober-Burkhardt, F. Wang, G. K. Surya Prakash, S. R. Narayanan, *J. Electrochem. Soc.* **2014**, *161*, A1371–A1380.
[10] a) W. T. Duan, R. S. Vemuri, J. D. Milshtein, S. Laramie, R. D. Dmello, J. H. Huang, L. Zhang, D. H. Hu, M. Vijayakumar, W. Wang, J. Liu, R. M. Darling, L. Thompson, K. Smith, J. S. Moore, F. R. Brushett, X. L. Wei, *J. Mater. Chem. A* **2016**, *4*, 5448–5456; b) R. A. Potash, J. R. McKone, S. Conte, H. D. Abruna, *J. Electrochem. Soc.* **2016**, *163*, A338–A344.
[11] a) Y. L. Liang, Z. L. Tao, J. Chen, *Adv. Energy Mater.* **2012**, *2*, 742–769; b) H. Nishide, K. Koshika, K. Oyaizu, *Pure Appl. Chem.* **2009**, *81*, 1961–1970; c) T. Janoschka, M. D. Hager, U. S. Schubert, *Adv. Mater.* **2012**, *24*, 6397–6409; d) P. Novák, K. Müller, K. S. V. Santhanam, O. Haas, *Chem. Rev.* **1997**, *97*, 207–281; e) Z. P. Song, H. S. Zhou, *Energy Environ. Sci.* **2013**, *6*, 2280–2301; f) P. Wardman, *J. Phys. Chem. Ref. Data* **1989**, *18*, 1637–1755; g) S. Muench, A. Wild, C. Friebe, B. Häupler, T. Janoschka, U. S. Schubert, *Chem. Rev.* **2016**, *116*, 9438–9484.
[12] T. Janoschka, N. Martin, U. Martin, C. Friebe, S. Morgenstern, H. Hiller, M. D. Hager, U. S. Schubert, *Nature* **2015**, *527*, 78–81.
[13] Y. Kato, Y. Shimizu, Y. J. Lin, K. Unoura, H. Utsumi, T. Ogata, *Electrochim. Acta* **1995**, *40*, 2799–2802.
[14] C. Lee, M. S. Moon, J. W. Park, *J. Inclusion Phenom.* **1996**, *26*, 219–232.

Received: November 25, 2016
Revised: December 21, 2016
Published online on February 7, 2017

